

The Inhibitive Effect of Poly(*p*-toluidine) on Corrosion of Iron in 1M HCl Solutions

P. Manivel,¹ G. Venkatachari²

¹A.C. College of Engineering and Technology, Karaikudi 630 004, Tamil Nadu, India

²Central Electrochemical Research Institute, Karaikudi 630003, Tamil Nadu, India

Received 19 September 2006; accepted 5 November 2006

DOI 10.1002/app.25838

Published online 16 February 2007 in Wiley InterScience (www.interscience.wiley.com).

ABSTRACT: In recent years, polymer amines have been recognized as an excellent corrosion inhibitors for iron in acid solutions. In this work, the inhibitive effect of *p*-toluidine and poly(*p*-toluidine) on corrosion of iron in 1M HCl has been studied by the electrochemical methods such as impedance, linear polarization, Tafel polarization techniques. The effectiveness of poly(*p*-toluidine) was found to be high in comparison with that of monomer. The results showed that *p*-toluidine and

poly(*p*-toluidine) suppressed both cathodic and anodic processes of iron dissolution in 1M HCl. The inhibition efficiency of both *p*-toluidine and poly(*p*-toluidine) were found to increase with the inhibitor concentrations. © 2007 Wiley Periodicals, Inc. *J Appl Polym Sci* 104: 2595–2601, 2007

Key words: *p*-toluidine; poly(*p*-toluidine); iron; HCl; inhibition; corrosion

INTRODUCTION

Acid inhibitors are widely used in chemical industries, acidizing of oil wells, cleaning of boilers, etc. The organic amine compounds are found to be more effective and highly efficient inhibitors due to the presence of nitrogen oxygen, sulfur, and π bonds in their structure. Many investigators^{1–4} have studied polyaniline, which was found to be an active inhibitor in hydrochloric acid solutions. It was found that a very small quantity of certain water soluble polymers was found to be effective in inhibiting the corrosion of iron.^{5–9}

Grchev et al.⁵ have found that poly(acrylic acid) and polyacrylamide were more effective on iron and gold in acid chloride solutions. Manivel and Venkatachari have studied the effect of poly(*p*-anisidine),⁶ poly(*p*-aminophenol),⁷ and poly(*p*-amino benzoic acid)⁸ in acid solutions and found that they were effective in 1M hydrochloric acid solutions. Sathyanarayanan et al.^{9,10} have studied the inhibitive properties of poly(*o*-methoxy aniline) and poly(*o*-ethoxy aniline) in acid solutions and found that they were effective in hydrochloric acid solutions. Kraljic et al.¹¹ investigated that the corrosion protection of stainless steel by electrochemically deposited poly-

aniline modified by addition of *o*-phenylene diamine found to be more effective.

Earlier studies^{4–12} have shown that the inhibitive properties of polyaniline and their derivatives on corrosion of iron in acid chloride solutions are due to the presence of π electrons, quaternary nitrogen atom and the larger molecular size which ensures greater coverage of the metallic surface. So the adsorption of polymer molecules on the iron electrode surface is more, which leads to more inhibition efficiency. Since a very few studies have been made on water soluble polymer amines, in this work, the inhibitive behavior of poly(*p*-toluidine) on iron in 1M HCl solution has been studied in comparison with that of monomer.

EXPERIMENTAL

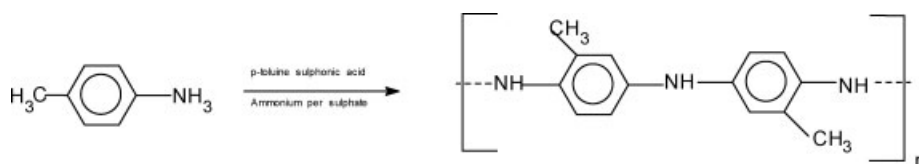
Preparation of polymer

Reagent grade *p*-toluidine was used for the preparation of water soluble poly(*p*-toluidine). A fresh solution of 0.1M *p*-toluene sulfonic acid was prepared using double distilled water. To this solution, 0.1M of *p*-toluidine dissolved in 0.1M HCl, was added and cooled to 0.5°C in a bath of ice and salt mixture. To this solution, freshly prepared solution of 0.1M Ammonium per sulfate was added slowly (to avoid warming) with constant stirring. The temperature was maintained below 5°C by the addition of crushed ice and stirring was continued for 2 h, to ensure the completion of reactions. The obtained polymer was characterized by FTIR and UV spectra,

Correspondence to: P. Manivel (mani_accet@yahoo.co.in).

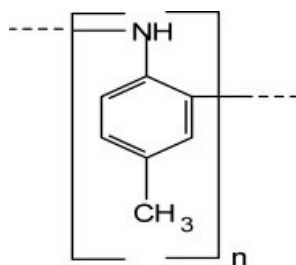
and the molecular weight determination was carried out by GPC. The average molecular weight of the

above polymer was found to be 7773. The formation of poly(*p*-toluidine) is given as follows.



Characterization of poly(*p*-toluidine)

The absorption peak at 260 nm shows the π - π^* transition in the benzenoid ring. The cation radicals and localized polaron peaks were observed at 360 nm and at 420 nm (Fig. 1). The major IR absorption bands at 1558 cm^{-1} and 1516 cm^{-1} are the characteristic bands due to nitrogen benzenoid ring structure (Fig. 2). The peak at 3236 cm^{-1} indicates N-H stretching and the IR absorption band 1635 cm^{-1} indicates the substitution for poly(*p*-toluidine) monomer unit at 1,4 positions. The other characteristic peaks for amino polymers observed at 1482 cm^{-1} , 1400 cm^{-1} , 1354 cm^{-1} , 1287 cm^{-1} , 1191 cm^{-1} , 1123 cm^{-1} , 1055 cm^{-1} , 1008 cm^{-1} , and 883 cm^{-1} . The structure of poly(*p*-toluidine) is as shown below.



Poly *p*-toluidine

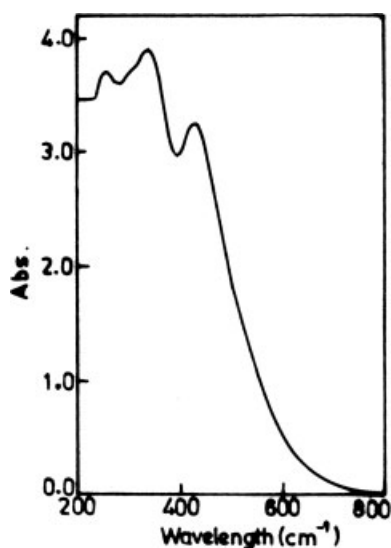


Figure 1 UV-visible spectrum for poly(*p*-toluidine).

Methodology

The electrochemical studies were carried out using a double walled glass cell having provisions for the working electrode, counter platinum electrode and luggin capillary as shown in Figure 3. The potential of the working electrode was measured with respect to saturated calomel electrode (SCE) through the luggin capillary. The working electrode was a pure iron (99.998%) and it was embedded in Araldite, so as to expose the surface area of 1 cm^2 . The electrode was polished with different grades of emery papers, and then degreased with trichloroethylene. The experiments were carried out after the steady state attainment of corrosion potentials (20 m) at $(30 \pm 1)^\circ\text{C}$. All the solutions were prepared using AR grade chemicals in double distilled water.

The impedance and polarization experiments were carried out using Solartron Electrochemical Analyser (model 1280B) with a software package of Z plot 2 and Corr ware 2. The impedance measurements were carried out at corrosion potential with the A.C. amplitude of 20 mV for the frequency range of 10 kHz to 10 mHz. The real and imaginary parts of the impedance were plotted in Nyquist plots. From the Nyquist plots, the charge transfer resistance (R_{ct}) and double layer capacitance (C_{dl}) values were calculated. The inhibitor efficiency

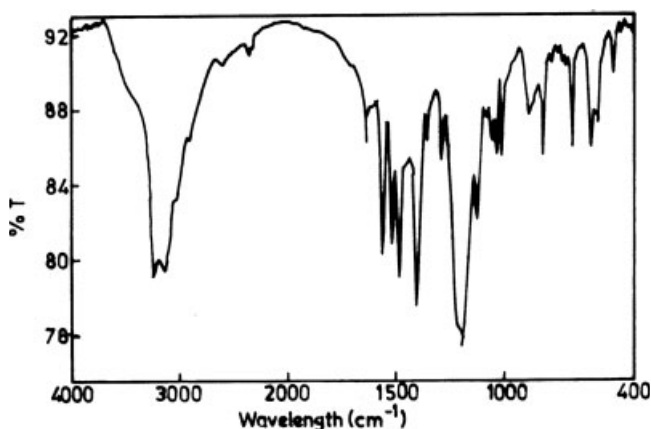


Figure 2 FTIR spectrum for poly(*p*-toluidine).

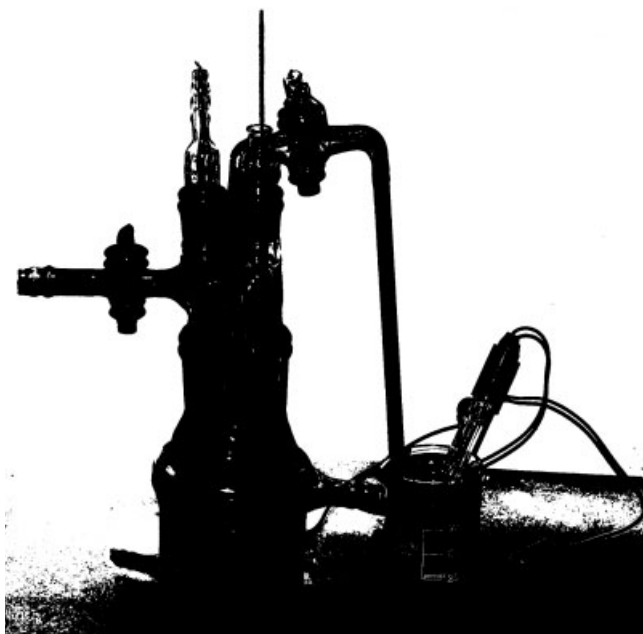


Figure 3 Polarization cell.

(I.E.) was calculated from R_{ct} values using the following equation:

$$\text{I.E. (\%)} = \frac{R_{ct(i)} - R_{ct}}{R_{ct(i)}} \quad (1)$$

where R_{ct} and $R_{ct(i)}$ are charge transfer resistance values in the absence and presence of inhibitor. The surface coverage (θ) values were calculated from the C_{dl} values using the following equation:

$$\theta = \frac{C_{dl} - C_{dl(i)}}{C_{dl}} \quad (2)$$

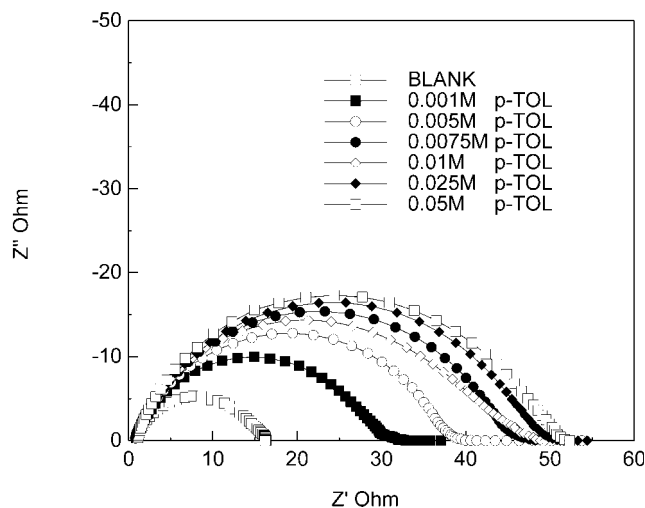


Figure 4 Nyquist plots of iron in 1M HCl with different concentrations of *p*-toluidine.

TABLE I
Electrochemical Parameters of Iron in 1M HCl without and with Different Concentrations of *p*-Toluidine

| Concentration (molar) | R_{ct} ($\Omega \text{ cm}^2$) | C_{dl} ($\mu\text{F}/\text{cm}^2$) | %I.E. | Surface coverage (θ) |
|-----------------------|------------------------------------|--|-------|-------------------------------|
| Nil | 15.6 | 330.1 | — | — |
| 1×10^{-3} | 32.2 | 148.3 | 51.6 | 0.55 |
| 5×10^{-3} | 39.6 | 148.3 | 60.7 | 0.55 |
| 7.5×10^{-3} | 45.4 | 127.1 | 65.7 | 0.61 |
| 1×10^{-2} | 47.6 | 107.7 | 67.3 | 0.67 |
| 2.5×10^{-2} | 49.9 | 107.6 | 68.8 | 0.67 |
| 5.0×10^{-2} | 54.1 | 108.6 | 71.3 | 0.67 |

where, C_{dl} and $C_{dl(i)}$ were the capacitance values in the absence and presence of inhibitors.

For linear polarization resistance studies, the measurements were carried out within the potential range of -15 mV to $+15 \text{ mV}$ with respect to open circuit potential and the current response was measured at a scan rate of 1 mV/s . The E and i data were plotted in a linear scale to get LPR plots and the slope of the plots gave the polarization resistance (R_p). The inhibitor efficiency (I.E.) was calculated R_p values using the following equation:

$$\text{I.E. (\%)} = \frac{R_{p(i)} - R_p}{R_{p(i)}} 100 \quad (3)$$

where R_p and $R_{p(i)}$ are the polarization resistance values in the absence and presence of inhibitor.

For potentiodynamic polarization studies, the experiments were carried out over a potential range of -200 mV to $+200 \text{ mV}$ with respect to open circuit potential at a scan rate of 1 mV/s . The various

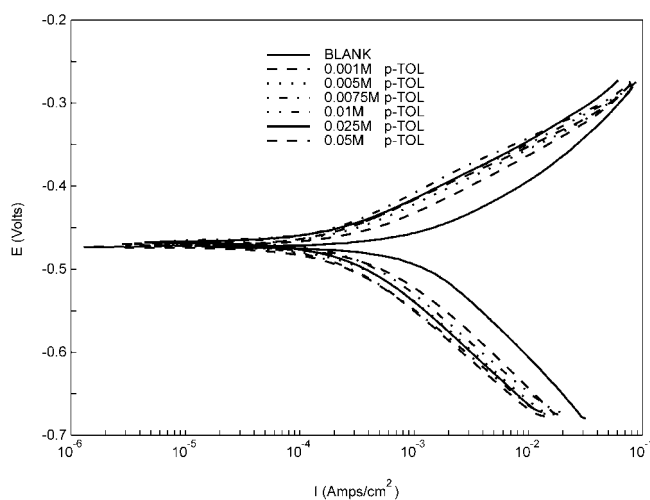


Figure 5 Polarization curves of iron in 1M HCl with different concentrations of *p*-toluidine.

TABLE II
Electrochemical Parameters of Iron in 1M HCl without and with Different Concentrations of *p*-Toluidine

| Concentration (molar) | E_{corr} (mV) | R_p ($\Omega \text{ cm}^2$) | %I.E. | b_a (mV) | b_c (mV) | I_{corr} ($\mu\text{A}/\text{cm}^2$) | %I.E. |
|-----------------------|------------------------|---------------------------------|-------|------------|------------|---|-------|
| Nil | -488.4 | 17.4 | - | 99.7 | 133.1 | 1425.5 | - |
| 1×10^{-3} | -475.5 | 49.2 | 64.7 | 74.2 | 120.1 | 472.3 | 66.9 |
| 5×10^{-3} | -474.5 | 68.0 | 74.5 | 67.4 | 118.7 | 374.4 | 73.7 |
| 7.5×10^{-3} | -474.5 | 85.8 | 79.7 | 64.5 | 116.5 | 269.9 | 81.1 |
| 1×10^{-2} | -474.8 | 92.5 | 81.2 | 65.9 | 111.1 | 256.9 | 82.0 |
| 2.5×10^{-2} | -472.3 | 69.0 | 74.8 | 67.3 | 117.9 | 236.2 | 83.4 |
| 5.0×10^{-2} | -472.1 | 79.9 | 78.2 | 72.1 | 120.7 | 227.9 | 84.0 |

kinetic parameters such as i_{corr} , b_a and b_c have been obtained from the polarization curves. The inhibitor efficiency (I.E.) was calculated from the i_{corr} values using the following equations,

$$\text{I.E. \%} = \frac{i_{\text{corr}} - i_{\text{corr}(i)}}{i_{\text{corr}}} 100 \quad (4)$$

where i_{corr} and $i_{\text{corr}(i)}$ are the corrosion current in the absence and presence of inhibitor.

RESULTS AND DISCUSSION

Inhibition by *p*-toluidine

The impedance measurements for iron in 1M HCl and 1M HCl with different concentrations of *p*-toluidine in the concentration range $1 \times 10^{-3}M$ to $5 \times 10^{-2}M$. Figure 4 shows the Nyquist plots for iron in 1M HCl containing *p*-toluidine. The charge transfer resistance (R_{ct}) values, the double layer capacitance (C_{dl}) values, and surface coverage (θ) values calculated from the impedance diagrams are given in Table I. It is observed that the charge transfer resistance values are increased from $32.2 \Omega \text{ cm}^2$

to $54.1 \Omega \text{ cm}^2$ with increase of *p*-toluidine concentration from $1 \times 10^{-3}M$ to $5 \times 10^{-2}M$. The decrease of C_{dl} values from 148.3 to $108.6 \mu\text{F}/\text{cm}^2$ indicates the good surface adsorption of inhibitor. The maximum inhibition efficiency obtained for this inhibitor is 71.3% at 0.05M concentration.

The polarization behavior of iron in 1M HCl and 1M HCl containing *p*-toluidine is shown in Figure 5. The electrochemical parameters obtained from these plots are shown given in Table II. In linear polarization study, the polarization resistance (R_p) is increased from $49.2 \Omega \text{ cm}^2$ to $79.85 \Omega \text{ cm}^2$ with increase in efficiency from 64.7% to 78.2%, with increase in concentration of inhibitor. It is found that there is no significant variation in the E_{corr} values in the presence of inhibitors suggesting that this polymer behaves as mixed type of inhibitor. Further, it is observed that the i_{corr} values are decreased from 472.3 to $227.85 \mu\text{A}/\text{cm}^2$ with increase in concentration of *p*-toluidine. The I.E. value is also found to increase from 66.9% to 84.0%. It is observed that there is a steady increase of inhibitor efficiencies with concentration as observed in the impedance results.

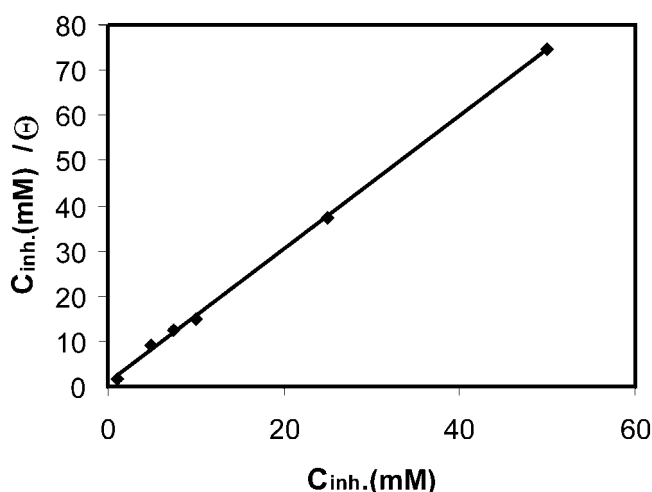


Figure 6 Langmuir isotherm plot for *p*-toluidine.

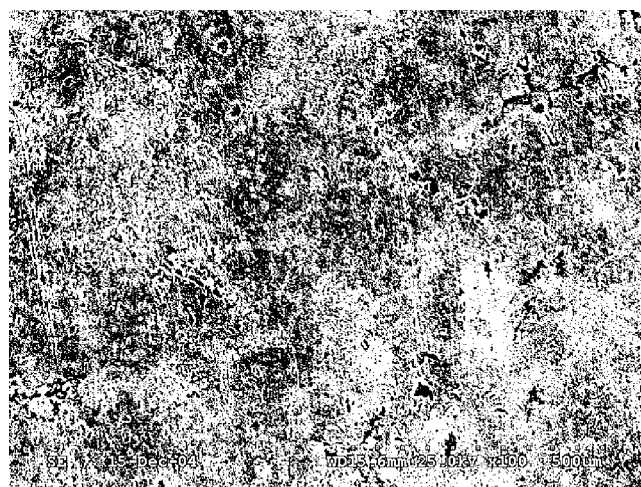


Figure 7 SEM photograph with ($\times 100$) magnification for iron in 1M HCl.

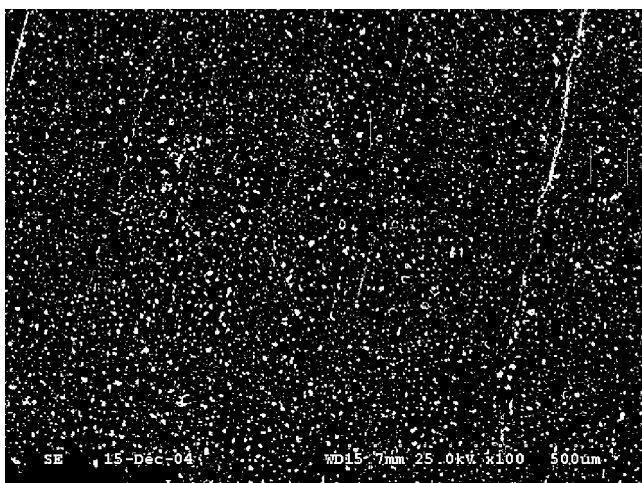


Figure 8 SEM photograph with ($\times 100$) magnification for iron in 1M HCl containing 0.05M *p*-toluidine.

Figure 6 shows the Langmuir adsorption isotherm plot of C_{inh} versus C_{inh}/θ , for *p*-toluidine. From this plot, it is observed that it obeys Langmuir adsorption isotherm through surface coverage of inhibitor adsorption on iron surface. The adsorption of the *p*-toluidine molecules with the metal surface is usually through the already adsorbed chloride ions. In acidic solutions, amines exist as cations and adsorb through electrostatic interaction between the positively charged anilinium cations and adsorbed chloride ions.¹²

The SEM photograph with (100 \times) magnification for iron in 1M HCl with and without presence of *p*-toluidine are given in Figures 7 and 8. It is observed from the photographs that the attack in presence of

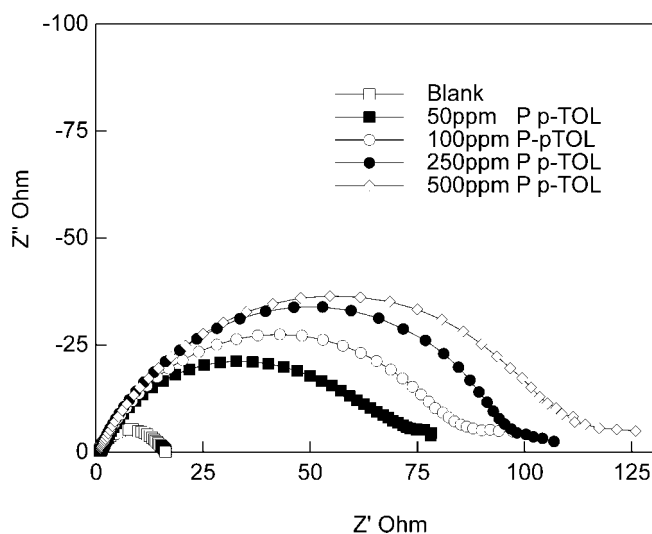


Figure 9 Nyquist plots of iron in 1M HCl with different concentrations of poly(*p*-toluidine).

TABLE III
Electrochemical Parameters of Iron in 1M HCl without and with Different Concentrations of Poly(*p*-toluidine)

| Concentration (ppm) | R_{ct} ($\Omega \text{ cm}^2$) | C_{dl} ($\mu\text{F}/\text{cm}^2$) | %I.E. | Surface coverage (θ) |
|---------------------|------------------------------------|--|-------|-------------------------------|
| Nil | 15.6 | 330.1 | – | – |
| 50 | 72.6 | 192.0 | 78.5 | 0.42 |
| 100 | 84.9 | 173.1 | 81.6 | 0.48 |
| 250 | 98.8 | 161.2 | 84.2 | 0.51 |
| 500 | 112.1 | 144.1 | 86.1 | 0.56 |

p-toluidine in 1M HCl is very less in comparison with the attack in absence of inhibitor in 1M HCl solution.

Inhibition by poly(*p*-toluidine)

The impedance studies for iron in 1M HCl containing poly(*p*-toluidine) in the concentration range 50 to 500 ppm are conducted. Figure 9 shows the Nyquist plots for iron in 1M HCl containing poly(*p*-toluidine). The charge transfer resistance (R_{ct}) values, the double layer capacitance (C_{dl}) values, and surface coverage (θ) values calculated from the impedance diagrams are given in Table III. It is found that the R_{ct} values are increased steadily from 72.6 to 112.1 $\Omega \text{ cm}^2$ with increase of inhibitor concentrations from 50 to 500 ppm. Also, it is observed that C_{dl} values are decreased from 192.0 to 144.1 $\mu\text{F}/\text{cm}^2$ with increase in concentration of inhibitor, which shows the inhibition is absorbed due to surface adsorption.

The polarization behavior of iron in 1M HCl containing poly(*p*-toluidine) is shown in Figure 10. The electrochemical parameters obtained from these dia-

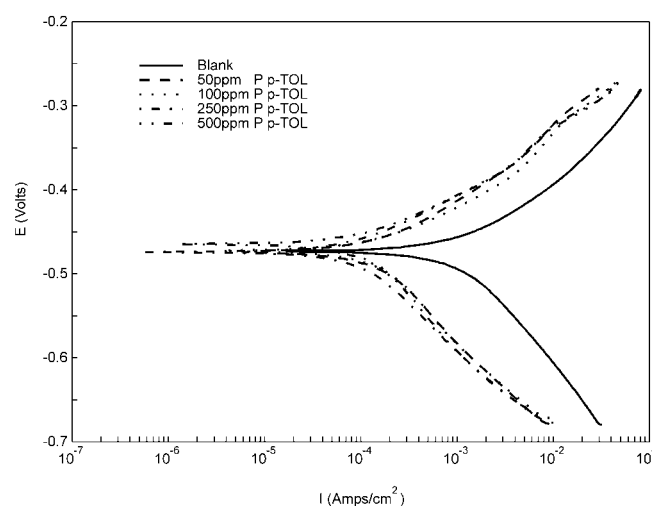


Figure 10 Polarization curves of iron in 1M HCl with different concentrations of poly(*p*-toluidine).

TABLE IV
Electrochemical Parameters of Iron in 1M HCl without and with Different Concentrations of Poly (*p*-toluidine)

| Concentration (ppm) | E_{corr} (mV) | R_p ($\Omega \text{ cm}^2$) | %I.E. | b_a (mV) | b_c (mV) | $I_{\text{corr.}}$ ($\mu\text{A}/\text{cm}^2$) | %I.E. |
|---------------------|------------------------|---------------------------------|-------|------------|------------|--|-------|
| Nil | -488.4 | 17.4 | - | 99.7 | 133.1 | 1425.5 | - |
| 50 | -479.7 | 100.5 | 82.7 | 70.6 | 128.1 | 137.1 | 90.3 |
| 100 | -479.0 | 111.1 | 84.3 | 58.1 | 32.7 | 130.6 | 90.8 |
| 250 | -473.1 | 138.1 | 87.4 | 57.5 | 116.6 | 83.9 | 94.1 |
| 500 | -472.5 | 130.6 | 86.7 | 53.3 | 111.5 | 76.6 | 94.6 |

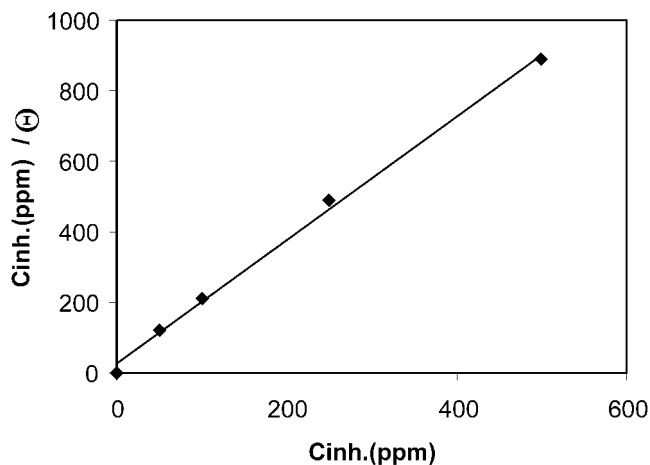


Figure 11 Langmuir isotherm plot for poly(*p*-toluidine).

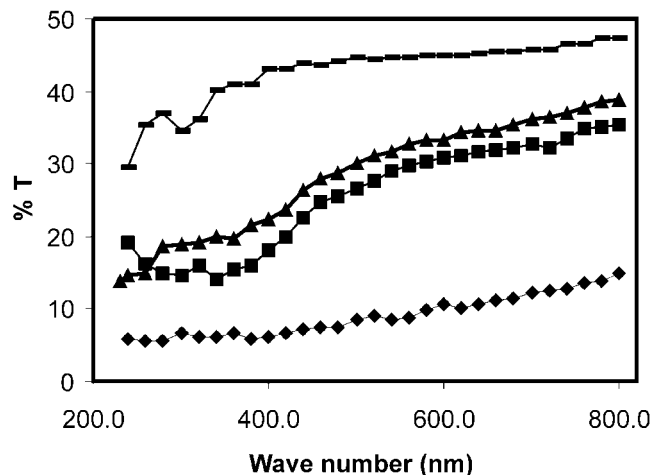


Figure 12 UV reflectance plot for poly(*p*-toluidine).

grams are shown given in Table IV. It is found that there is no significant variation in the E_{corr} values in the presence of inhibitors suggesting that this polymer behaves as mixed type of inhibitor. The inhibitor efficiency values calculated from linear polarization resistance (R_p) values are found to increase with increase in concentrations.

The Tafel slopes remained unaffected in the presence of inhibitor poly(*p*-toluidine). The i_{corr} values are found to decrease from 137.1 to 76.6 $\mu\text{A}/\text{cm}^2$ and it shows that there is a steady increase of inhibitor efficiencies with concentration. Figure 11 shows the adsorption isotherm [plot of C_{inh} versus C_{inh}/θ] for poly(*p*-toluidine). It is found that poly

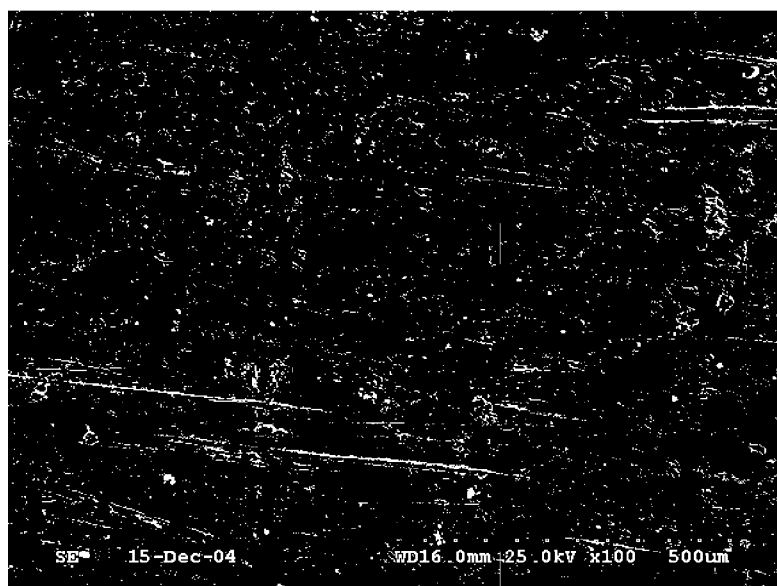


Figure 13 SEM photograph with ($\times 100$) magnification for iron in 1M HCl containing 500 ppm poly(*p*-toluidine).

(*p*-toluidine) obeys Langmuir isotherm. The higher inhibitive property of poly(*p*-toluidine) is also due to the presence of π electrons, quaternary nitrogen atom and the larger molecular size which ensures greater coverage of the metallic surface.⁶⁻¹⁶ Similarly the reflectance study (Fig. 12) indicates the more protective nature of poly(*p*-toluidine) than that of monomer.

The SEM photograph with (100 \times) magnification for iron in 1M HCl containing 500 ppm poly(*p*-toluidine) is given in Figure 13. It is seen from the photograph that the attack in presence of 500 ppm poly(*p*-toluidine) in 1M HCl is very less in comparison with that of monomer in 1M HCl solution.

CONCLUSIONS

1. The inhibition efficiency for both monomer and polymer of *p*-toluidine increases with increase in concentrations.
2. Poly(*p*-toluidine) has shown a better performance of inhibition efficiency for iron in 1M HCl solutions when compared with its monomer.
3. Both *p*-toluidine and poly(*p*-toluidine) were found to be mixed type of inhibitor.
4. The adsorption of both monomer and polymer of *p*-toluidine on iron surface in 1M HCl obey Langmuir adsorption isotherm.

References

1. Hatchett, D. W.; Josowicz, M.; Janata, J. J Electrochem Soc 1999, 146, 4535.
2. Maeda, Y.; Kabsuta, A.; Nagasaki, K.; Kamiyama, M. J Electrochem Soc 1995, 142, 2261.
3. Tang, H.; Kitani, A.; Shiotani, M. Electrochim Acta 1996, 41, 1561.
4. Wei, X. L.; Wang, Y. Z.; Long, S. M.; Bobeczko, C.; Epstein, A. J. J Am Chem Soc 1996, 118, 2545.
5. Grchev, T.; Cvetkovska, M.; Schultze, J. W. Corrosion Sci 1991, 32, 103.
6. Manivel, P.; Venkatachari, G. Corrosion Sci Technol 2005, 4, 51.
7. Manivel, P.; Venkatachari, G. J Met Mater Sci 2004, 46, 165.
8. Manivel, P.; Venkatachari, G. J Mater Sci Technol 2006, 22, 301.
9. Sathyanarayanan, S.; Dhawan, S. K.; Trivedi, D. C.; Balakrishnan, K. Corrosion Sci 1992, 33, 1831.
10. Sathyanarayanan, S.; Balakrishnan, K.; Dhawan, S. K.; Trivedi, D. C. Electrochim Acta 1994, 39, 831.
11. Kraljic, M.; Zic, M.; Duic, L. Bull Electrochem 2004, 20, 567.
12. Gerovich, M. A.; Rybalchenko, G. F. Zh Fiz Khim 1958, 32, 109.
13. Khalad, K. F.; Hackerman, N. Electrochim Acta 2003, 48, 2715.
14. Bentiss, F.; Traisnel, M.; Lagnee, M. J Appl Electrochem 2001, 31, 41.
15. Ramesh Babu, B.; Holze, R. Br Corrosion J 2000, 35, 204.
16. Manivel, P.; Venkatachari, G. J Met Mater Sci 2004, 46, 263.